Role of Domain Interactions in the Collective Motion of Phosphoglycerate Kinase

Gusztáv Schay, Levente Herényi, Judit Fidy, and Szabolcs Osváth*
Department of Biophysics and Radiation Biology, Semmelweis University, Budapest, Hungary

ABSTRACT Protein function is governed by the underlying conformational dynamics of the molecule. The experimental and theoretical work leading to contemporary understanding of enzyme dynamics was mostly restricted to the large-scale movements of single-domain proteins. Collective movements resulting from a regulatory interplay between protein domains is often crucial for enzymatic activity. It is not clear, however, how our knowledge could be extended to describe collective near-equilibrium motions of multidomain enzymes. We examined the effect of domain interactions on the low temperature near equilibrium dynamics of the native state, using phosphoglycerate kinase as model protein. We measured thermal activation of tryptophan phosphorescence quenching to explore millisecond-range protein motions. The two protein domains of phosphoglycerate kinase correspond to two dynamic units, but interdomain interactions link the motion of the two domains. The effect of the interdomain interactions on the activation of motions in the individual domains is asymmetric. As the temperature of the frozen protein is increased from the cryogenic, motions of the N domain are activated first. This is a partial activation, however, and the full dynamics of the domain becomes activated only after the activation of the C domain.

INTRODUCTION

Conformational dynamics of proteins is of fundamental importance for their biological function. Protein dynamics, however, is a complex phenomenon, involving hierarchical networks of motions spanning several orders of magnitude in time and space. The timescales may extend from picoseconds to seconds, and important motions could range from small local vibrations to large conformational changes, or small collective motions affecting the entire protein (1–3). Some dynamic components are observable even at cryogenic temperatures, whereas others require more thermal activation (1,4).

Tryptophan phosphorescence lifetime measurements allow studying internal dynamics of proteins in the millisecond range (5–7). Phosphorescence lifetime is sensitive to changes in protein structure, flexibility, or structure fluctuations, due to quenching by internal amino-acid residues or external quencher molecules (8,9). One almost ubiquitous quencher of tryptophan phosphorescence is oxygen (7). It has been shown, however, that the collisional quenching with oxygen molecules can be used to study the activation of the low temperature dynamics of proteins (1).

Due to the obvious advantage of simplicity, most of the experimental and theoretical work leading to contemporary understanding of enzyme function and dynamics was restricted to the large-scale movements of small single-domain proteins (3,4,10). These studies contributed significantly to our understanding of the biological role of protein dynamics. It is clear, however, that our knowledge should be extended to describe large multidomain proteins, and to understand the importance of collective near-equilibrium motions.

Yeast 3-phosphoglycerate kinase (PGK) is a typical two-domain hinge-bending enzyme with a conserved primary structure and tertiary fold including a well-structured interdomain region (11,12). The two domains interact via a helical hinge and through the C-terminal helix, which folds back to the N domain, and proved to be crucial for enzyme activity (12,13). Contacts between the two domains are formed through hydrophobic interactions and hydrogen bonds in the folded structure (14,15). These contacts bear extreme importance in the ligand-influenced conformational change: a hinge-bending motion of the entire protein (16–18). There are two tryptophan residues in the wild-type yeast PGK that can serve as luminescent probes of the protein conformation (5,19,20). Folding of fragments containing less than one structural domain is incomplete and not cooperative, but both individual full-length domains fold into nativelike structures (21,22). PGK therefore is a suitable model to study the mechanism of domain-domain interplay and its role in protein dynamics.

In this article, we use PGK as a model to clarify the effect of the domain interactions on the small near-equilibrium collective motion of multidomain proteins.

MATERIALS AND METHODS

Mutants of histidine-tagged PGK, histidine-tagged N domain of PGK, and histidine-tagged C domain of PGK were expressed using T7 promoter in Rosetta cells (a codon-plus variant of *Escherichia coli* BL-21). Aliquots (5 mL) of overnight LB cultures started from single cell colonies were used to inoculate 1 L 2×YT media. All cultures contained 34 mg/L chloramphenicol and 30 mg/L kanamycin. After 4 h of growth in a shaker at 37°C, protein expression was induced by the addition of 1 mM isopropyl β-D-1-thiogalactopyranoside, and then growth was continued

Submitted June 26, 2012, and accepted for publication December 13, 2012.

*Correspondence: szabolcs.osvath@eok.sote.hu

Editor: Catherine Royer.

0006-3495/13/02/0677/6 $2.00

http://dx.doi.org/10.1016/j.bpj.2012.12.025

under the same conditions for another 4 h. Cells were harvested by centrifugation, flash-frozen in liquid nitrogen, and stored at –80°C until further use (23,24).

His-affinity protein purification was done on Ni-NTA column (Qiagen, Germantown, MD). After the addition of roughly 0.3 mg 4-(2-aminoethyl) benzenesulfonyl fluoride hydrochloride per 60 g wet cell weight, cells were lysed by sonication. The His-tagged target protein was purified according to Qiagen's nondenaturing protocol. PGK mutants were eluted between 25 and 40 mM imidazole. The fractions collected were checked for protein content and purity by denaturing polyacrylamide gel electrophoresis. The cleanest fractions were pooled and concentrated to 30 μM by ultrafiltration, extensively dialyzed at 4°C against 20 mM phosphate buffer (pH 7.0), centrifuged for 20 min at 20,000g to remove any precipitate, flash-frozen in liquid nitrogen, and stored at –80°C (23,24). Protein concentrations were determined using the method of Edelhoch (25) from the ultraviolet absorbance spectra measured on a Carry4E spectrophotometer. A detailed assay indicates stable formation of the native structure in the proteins studied in this article (24,26,27).

Thermal activation of phosphorescence quenching was measured in oxygen-saturated aqueous protein solutions. Fast cooling of the sample to the target temperature and ensuring thermodynamic equilibrium at the target temperature were critical. Samples containing 20 μM protein, 20 mM potassium phosphate (pH 6.2), and 1 mM ethylenediaminetetraacetic acid (EDTA) were flash-frozen, and then equilibrated for 4 h at 8 K before starting a measurement. After this, samples were gradually heated in 5 K or 10 K steps and allowed to equilibrate for 45 min at the target temperature before recording the phosphorescence lifetime. As we have shown in an earlier publication that introduced the technique used in this article, fast cooling is very important to preserve native protein structure (1). The cooling and warming protocol was double-checked by measuring the enzymatic activity of the N*C and NC* proteins after a temperature cycle. No significant loss of enzymatic activity was observed. Assuring that measurements are done after reaching thermodynamic equilibrium is also very important. To verify that measurements are done in thermal equilibrium, three consecutive measurements were done at selected temperatures. For each measurement, 700 traces were averaged. Because averaging 700 traces lasted $>$ 8 h, recording the three curves lasted more than one day. No significant difference was found between the three curves, which suggests that the sample was sufficiently equilibrated before the measurement.

Intrinsic tryptophan phosphorescence of the protein samples was measured using the time-domain mode of an EAI CD900 spectrometer (Edinburgh Analytical Instruments, Edinburgh, UK) equipped with a μF900 Xe flash-lamp (1 mJ/pulse, 2 μs full-width at half-maximum). Samples were excited at 290 nm (5-nm spectral width) and luminescence was detected at 421 nm (5-nm spectral width). Phosphorescence emission signals were weak due to light scattering and quenching effects. To reach an acceptable signal/noise ratio, 700 consecutive traces were summed with 80-μs time resolution.

As we showed earlier, the average lifetime of the phosphorescence decay can be used to describe the millisecond range dynamics of the protein (1). Phosphorescence decay curves were fit with a distribution of exponentials using the maximum entropy method described by Bryan (28). This procedure fitted the decays with 100 exponential components that were equally spaced on a logarithmic timescale. The average phosphorescence lifetimes were calculated from the distribution using the formula

$$\langle \tau \rangle = \frac{\sum_{i=1}^{n} A_i \tau_i^2}{\sum_{i=1}^{n} A_i \tau_i},$$

where n is the number of exponential components present in the phosphorescence decay and A_i is the amplitude of the decay component with τ_i characteristic time.

RESULTS

A model system based on the two-domain structure of PGK was constructed to study the role of domain interactions on the near-equilibrium dynamics of proteins. Sequence differences between the mutants and the wild-type protein are summarized in Table 1. In this article, we use the following notation: N, C, and NC refer to the N-terminal domain, the C-terminal domain, and the full sequence containing both domains of the PGK structure, respectively. The model protein system consists of four mutants that contain a single tryptophan residue. An asterisk (*) sign indicates the domain on which the luminescent probe is located.

The four mutants are logically organized in two pairs. Both pairs contain one individual domain (either the N- or the C-terminal domain) and a corresponding mutant of the intact protein. Within the pair, the single tryptophan residues are placed at identical positions. Tryptophan phosphorescence allowed selective detection of millisecond-timescale motions inside the domains of PGK both in the presence and in the absence of domain interactions. Fig. 1 *a* represents phosphorescence decay curves of the N* and C* proteins at 8 K. Phosphorescence decay traces were fitted with a distribution of lifetimes. Fig. 1 *b* shows the fraction of phosphorescent molecules as a function of the phosphorescence lifetime.

Phosphorescence decay curves were recorded at several temperatures between 8 and 273 K. Fig. 2 *a* shows three phosphorescence decay traces of NC* measured at three different temperatures. As temperature is increased from 8 K, protein movements are gradually activated. Motions allow faster oxygen diffusion, which facilitates phosphorescence quenching, shortening the average phosphorescence lifetime as it can be seen in Fig. 2 *b*.

Phosphorescence decay curves of all four mutants were recorded between 8 and 273 K and analyzed as described above. Decays observed on the C* and NC* mutants were found to be more heterogeneous than the decay measured on the N* and N*C proteins. Fig. 3 shows the temperature dependence of the average tryptophan phosphorescence decay times for the four mutants of the model protein system.

DISCUSSION

Dynamic quenching by the protein matrix and by the oxygen molecules both can influence observed tryptophan

TABLE 1 Sequence differences between the mutants of the protein system and the wild-type PGK

Construct	Sequence length	Position of the single Trp	Mutations compared to the wild-type PGK
N*	Residues 1–185	W122	Stop after residue 185, Y122W
N*C	Full PGK sequence	W122	Y122W, W308F, W333F
C*	Residues 186–415	W333	Start at residue 186, W308F
NC*	Full PGK sequence	W333	W308F

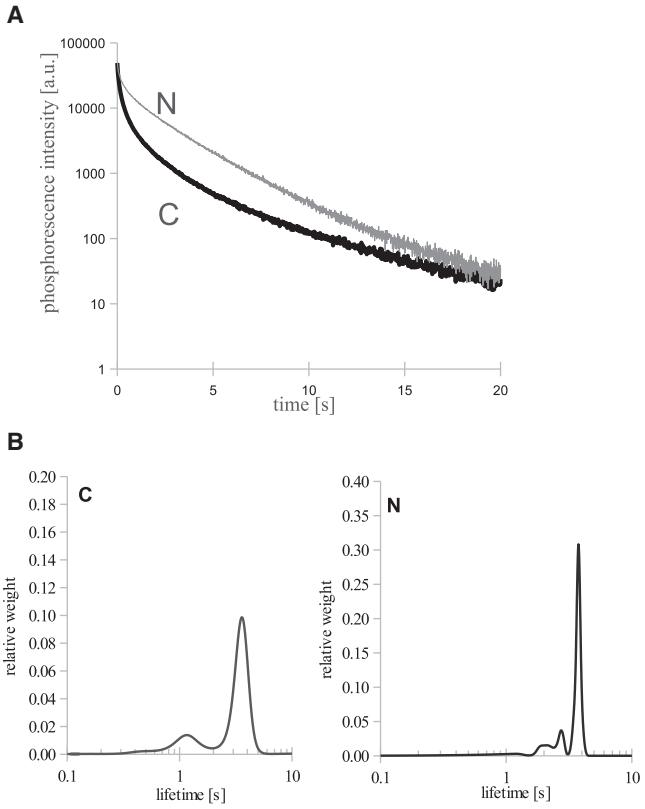

FIGURE 1 Phosphorescence lifetimes of the N* and C* proteins. (*A*) Phosphorescence decay traces recorded at 8 K after flash excitation of the sample. (*B*) Probability density distribution of the phosphorescence lifetimes in the N* and C* protein molecules. Samples contained 20 μM protein, 20 mM potassium phosphate (pH 6.2), and 1 mM EDTA.

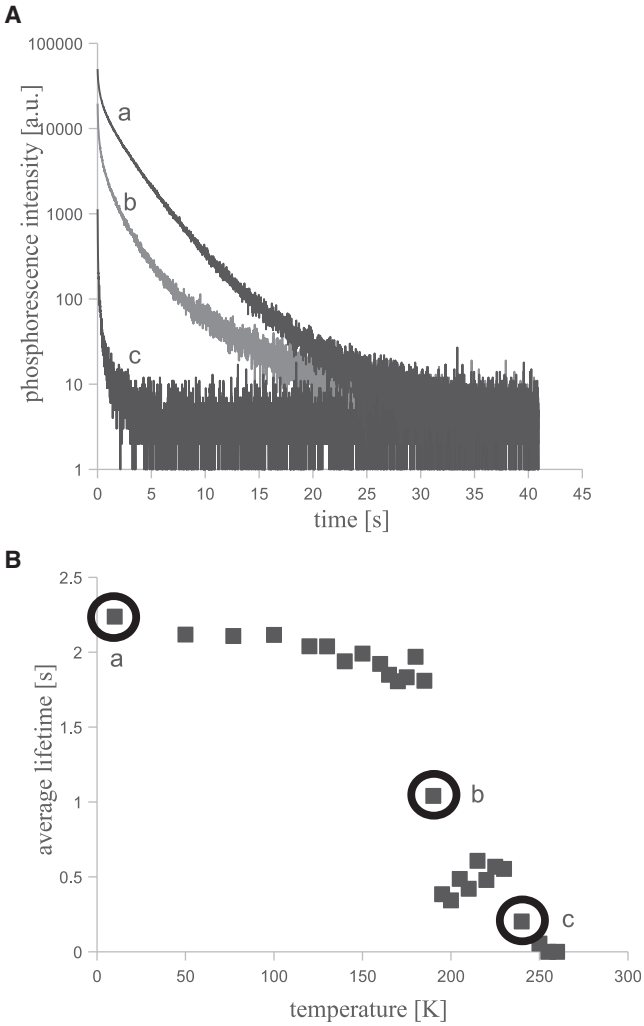

FIGURE 2 Temperature dependence of the phosphorescence decay of the NC* protein. (*A*) Phosphorescence decay traces of NC* protein measured at 8 K, 190 K, and 240 K. (*B*) Temperature dependence of the average phosphorescence lifetime of the NC* protein. Samples contained 20 μM protein, 20 mM potassium phosphate (pH 6.2), and 1 mM EDTA.

phosphorescence lifetime of proteins. In the presence of oxygen, however, quenching by the oxygen molecules is dominant (7). Oxygen-depleted samples show a much smaller phosphorescence lifetime change, which is distributed over a broader temperature range (1). Also, most of the lifetime change of oxygen-depleted samples happens above the temperature where the transitions described in this article were found. The internal motions within the protein are strongly related to the diffusion of oxygen, thus quenching by oxygen can be used to assay thermal activation of near-equilibrium protein movements.

A thermodynamic model was developed to account for the activation of the intramolecular motions that lead to tryptophan phosphorescence quenching. The model assumes that the protein can exist in two different states. In the lower energy state, global movements of the protein are frozen. The average tryptophan phosphorescence lifetime is the intrinsic lifetime $\langle\tau_0\rangle$, which is an ensemble average. Global protein motions that result in phosphorescence quenching require thermal activation and correspond to a state with higher energy. In this state, the average tryptophan phosphorescence lifetime $\langle\tau_d\rangle$ is smaller than $\langle\tau_0\rangle$ due to quenching by collision with oxygen molecules diffusing within the protein matrix. A quenching factor K_d can be defined that describes the strength of the quenching occurring due to collision with oxygen:

$$K_d = \frac{\langle\tau_0\rangle}{\langle\tau_d\rangle}.$$

If the states with activated and frozen movements are both populated, the average phosphorescence lifetime can be calculated as

$$\langle\tau\rangle = n_0\langle\tau_0\rangle + n_d\langle\tau_d\rangle,$$

where n_d is the fraction of protein molecules in which motions are activated, and n_0 is the fraction of molecules in which motions are frozen.

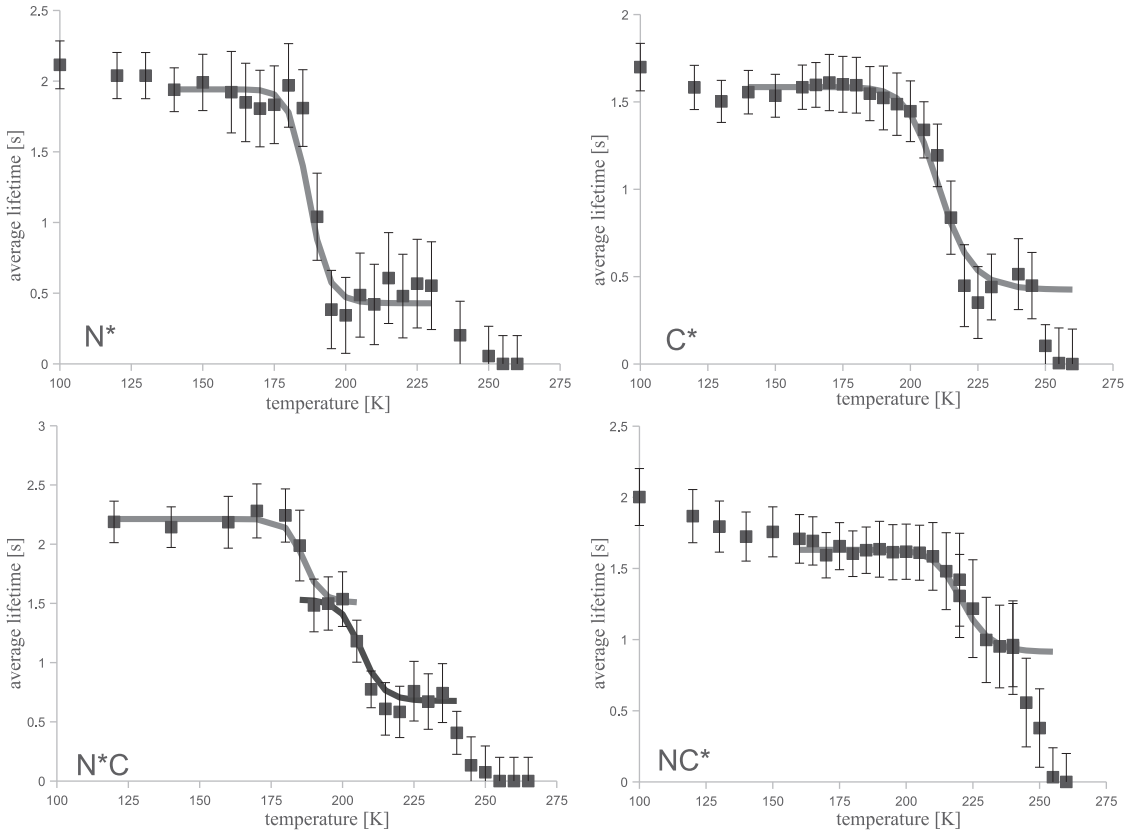

FIGURE 3 Temperature dependence of the average phosphorescence lifetime of the N*, C*, N*C, and NC* proteins. (*Continuous lines*) Average phosphorescence lifetimes obtained using the thermodynamic model for activation of protein motions described in the text with the activation parameters summarized in Table 2. Samples contained 20 μM protein, 20 mM potassium phosphate (pH 6.2), and 1 mM EDTA.

The ratio of n_d and n_0 can be calculated from the free energy difference between the two states:

$$\frac{n_d}{n_0} = e^{\frac{-(\Delta E - T\Delta S)}{kT}}.$$

Here ΔE is the energy difference between the two states; ΔS is the entropy difference between the two states; T is the absolute temperature; and k is Boltzmann's constant.

The $\Delta E - T\Delta S$ term gives the free energy difference between the two states. As the temperature is increased, the entropic term increases, and the free energy difference decreases. At the midpoint temperature (T_{MP}), the free energy of the two states becomes equal:

$$\Delta E - T_{MP}\Delta S = 0,$$

thus

$$T_{MP} = \frac{\Delta E}{\Delta S}.$$

The two states are equally populated ($n_d = n_0$) at the midpoint temperature. Above the midpoint temperature, the state in which global motions are activated is more populated than the state in which global motions are frozen ($n_d > n_0$).

Continuous lines in Fig. 3 indicate fitted average lifetimes as a function of temperature, calculated using the above model. The corresponding activation parameters are summarized in Table 2.

The magnitude of the energy differences in Table 2 is comparable to the energy of a few hydrogen bonds. The entropy change is comparable to the denaturation entropy of ~2–5 amino-acid residues (29). Based on these values, we speculate that the thermally activated quenching by collisions with oxygen molecules involves an average hopping distance (mean free path) of a length of a few (~2–5) amino-acid residues. Collisional quenching is made possible

TABLE 2 Activation parameters of the motions leading to phosphorescence quenching

	ΔE (kJ·mol−1)	ΔS (J·mol−1·K−1)	TMP (K)	Kd	$\langle\tau 0\rangle$ (s)
N*	84.4 ± 6.7	445 ± 36	189 ± 5.1	4.7 ± 0.3	2.24
N*C 1	92.1 ± 6.4	494 ± 35	186 ± 4.1	1.5 ± 0.2	2.52
N*C 2	—	—	207 ± 3.9	2.3 ± 0.2	
C*	61.7 ± 5.6	293 ± 26	211 ± 9.7	3.7 ± 0.3	1.84
NC*	74.5 ± 7.2	336 ± 24	222 ± 10.8	1.8 ± 0.2	2.27

by a limited anisotropic diffusion process inside the protein and in its coupled surroundings by hopping through transiently opening spaces, which are created locally by the global dynamics of the structure.

Fig. 3 shows that the activation of the dynamics is very different in the N*, C*, N*C, and NC* proteins. Our simple thermodynamic model, however, could describe the activation of the dynamics of all the four proteins. The model predicts well the phosphorescence lifetime changes of the N*, C*, N*C, and NC* proteins in the low temperature range, but an additional transition can also be observed at higher temperatures which was not included in the model. This additional transition is found at the same temperature for all four mutants and we attribute it to the softening of the solvent matrix surrounding the protein (1).

The transition temperature range in which molecular motions are activated is significantly broader for the C* protein than for the N* sample. The same holds for the NC* mutant, in which the dynamics becomes activated in such a broad range that it blends into the beginning of the transition corresponding to the softening of the surrounding matrix. A strikingly different curve was found for the N*C mutant in which the activation of the molecular dynamics is split into two steps. The T_{MP} of the first step coincides with the activation step found in N*, but the full curve of N*C indicates only partial activation of the motions at this temperature compared to the N* mutant. A second step follows closely after the first and it lowers the average lifetime to the value seen in N*. This two-step behavior is distinct from the single, broad transition of the NC* construct.

There is an asymmetry in the ΔE and ΔS activation parameters for the four proteins. The activation parameters differ significantly for the NC* and N*C mutants, and resemble the difference between the N* and C*. The activation energy and entropy values are larger in the full-length constructs than in the single domains in both pairs (N* versus N*C and C* versus NC*). This increase is ~10–15% for the C* versus NC*, and somewhat smaller in the case of the N* versus N*C pair. The first step of the activation of motions in the N*C protein can be fitted with a two-step model. Because our model works only for the activation from the frozen state, the ΔE and ΔS activation parameters could not be calculated for the second transition of N*C. The second transition was analyzed phenomenologically by fitting with a sigmoid curve to obtain the midpoint temperature of the transition (T_{MP}) and the K_d ratio. These characterize the activation of new motions within a second step as the protein is heated further. In such a more complex case, the transition midpoint temperature is a good parameter to compare the behavior of the mutants. The first transition midpoint temperature of the N*C corresponds to that of the single N-domain, while the second transition midpoint temperature of the N*C activation coincides with the transition temperature of the C and NC* proteins.

The high-resolution structure of PGK suggests that the two domains of the protein are largely independent (12). This partial autonomy of the domains is in accordance with our results and it is reflected in the activation parameters summarized in Table 2. The two domains, however, are not completely independent. It has been shown in other works that a network of interactions sets a balanced interplay between the two domains. This interplay facilitates a hinge-bending movement at physiological conditions, which is crucial for enzyme function (14). Here we found a strong coupling between the motion of the two domains at low temperatures, when large-scale motions are frozen, and hinge bending is not possible. This shows that hinge-bending motion is not the only result of interdomain communication: there is a collective dynamics of the two domains even when hinge bending is blocked. As temperature is increased from the cryogenic, activation of the N*C stops in a partially activated state waiting for the C-domain to become activated. Only the activation of the collective dynamics of the two domains allows quenching of the phosphorescence to the same extent as within the N* protein.

Our results suggest that the two domains of PGK correspond to two dynamic units of the native state. The motions of the two dynamic units, however, are coupled through domain-domain interactions. Apparently, the interaction between the two domains has an asymmetric effect on the activation of motion in the domains. This seems surprising, based on the symmetric structure of the PGK and the symmetric role of the domains in bringing the 1,3-phosphoglycerate and ADP together for phosphate transfer. Our results, however, are in accord with earlier findings indicating that domain-domain interactions also have asymmetric effect on the folding of the domains (27).

CONCLUSIONS

The two domains of PGK correspond to two dynamic units, but collective movements involving both domains also exist. Interdomain interactions play important role in the dynamic coupling of the two domains. The effect of the interdomain interactions on the activation of motions in the individual domains is asymmetric. Apparently, the hinge-bending motion is not essential for the interdomain communication: there is a collective dynamics of the two domains even when hinge bending is blocked. As the temperature of the frozen protein is increased from the cryogenic, motions of the N domain become activated first. This is a partial activation, however, and full movement of the domain becomes possible only after the activation of the C domain.

This work was funded by the Hungarian Scientific Research Fund under grants No. OTKA K-77730 and No. OTKA K-84271 and the János Bolyai Research Scholarship of the Hungarian Academy of Sciences under grant No. BO/00468/09.

REFERENCES

1. Schay, G., L. Herényi, …, J. Fidy. 2011. Millisecond time-scale protein dynamics exists prior to the activation of the bulk solvent matrix. *J. Phys. Chem. B.* 115:5707–5715.
2. Henzler-Wildman, K., and D. Kern. 2007. Dynamic personalities of proteins. *Nature.* 450:964–972.
3. Tzeng, S. R., and C. G. Kalodimos. 2011. Protein dynamics and allostery: an NMR view. *Curr. Opin. Struct. Biol.* 21:62–67.
4. Mittermaier, A., and L. E. Kay. 2006. New tools provide new insights in NMR studies of protein dynamics. *Science.* 312:224–228.
5. Cioni, P., and G. B. Strambini. 1994. Pressure effects on protein flexibility monomeric proteins. *J. Mol. Biol.* 242:291–301.
6. Papp, S., and J. M. Vanderkooi. 1989. Tryptophan phosphorescence at room temperature as a tool to study protein structure and dynamics. *Photochem. Photobiol.* 49:775–784.
7. Vanderkooi, J. M., D. B. Calhoun, and S. W. Englander. 1987. On the prevalence of room-temperature protein phosphorescence. *Science.* 236:568–569.
8. Strambini, G. B., and M. Gonnelli. 2010. Acrylonitrile quenching of Trp phosphorescence in proteins: a probe of the internal flexibility of the globular fold. *Biophys. J.* 99:944–952.
9. Cioni, P., E. de Waal, …, G. B. Strambini. 2004. Effects of cavity-forming mutations on the internal dynamics of azurin. *Biophys. J.* 86:1149–1159.
10. Gillespie, B., and K. W. Plaxco. 2004. Using protein folding rates to test protein folding theories. *Annu. Rev. Biochem.* 73:837–859.
11. Banks, R. D., C. C. Blake, …, A. W. Phillips. 1979. Sequence, structure and activity of phosphoglycerate kinase: a possible hinge-bending enzyme. *Nature.* 279:773–777.
12. Watson, H. C., N. P. Walker, …, S. M. Kingsman. 1982. Sequence and structure of yeast phosphoglycerate kinase. *EMBO J.* 1:1635–1640.
13. Ritco-Vonsovici, M., B. Mouratou, …, E. Guittet. 1995. Role of the C-terminal helix in the folding and stability of yeast phosphoglycerate kinase. *Biochemistry.* 34:833–841.
14. Varga, A., B. Flachner, …, M. Vas. 2005. Correlation between conformational stability of the ternary enzyme-substrate complex and domain closure of 3-phosphoglycerate kinase. *FEBS J.* 272:1867–1885.
15. Balog, E., M. Laberge, and J. Fidy. 2007. The influence of interdomain interactions on the intradomain motions in yeast phosphoglycerate kinase: a molecular dynamics study. *Biophys. J.* 92:1709–1716.
16. Guilbert, C., F. Pecorari, …, L. Mouawad. 1996. Low frequency motions in phosphoglycerate kinase. A normal mode analysis. *Chem. Phys.* 204:327–336.
17. Guilbert, C., D. Perahia, and L. Mouawad. 1995. A method to explore transition paths in macromolecules. Applications to hemoglobin and phosphoglycerate kinase. *Comput. Phys. Commun.* 91:263–273.
18. Vas, M., A. Varga, and E. Gráczer. 2010. Insight into the mechanism of domain movements and their role in enzyme function: example of 3-phosphoglycerate kinase. *Curr. Protein Pept. Sci.* 11:118–147.
19. Damaschun, G., H. Damaschun, …, D. Zirwer. 1998. Denatured states of yeast phosphoglycerate kinase. *Biochemistry* (*Mosc.*). 63:259–275.
20. Missiakas, D., J. M. Betton, …, J. M. Yon. 1990. Unfolding-refolding of the domains in yeast phosphoglycerate kinase: comparison with the isolated engineered domains. *Biochemistry.* 29:8683–8689.
21. Hosszu, L. L. P., C. J. Craven, …, J. P. Waltho. 1997. Is the structure of the N-domain of phosphoglycerate kinase affected by isolation from the intact molecule? *Biochemistry.* 36:333–340.
22. Pecorari, F., C. Guilbert, …, J. M. Yon. 1996. Folding and functional complementation of engineered fragments from yeast phosphoglycerate kinase. *Biochemistry.* 35:3465–3476.
23. Osváth, S., and M. Gruebele. 2003. Proline can have opposite effects on fast and slow protein folding phases. *Biophys. J.* 85:1215–1222.
24. Osváth, S., J. J. Sabelko, and M. Gruebele. 2003. Tuning the heterogeneous early folding dynamics of phosphoglycerate kinase. *J. Mol. Biol.* 333:187–199.
25. Edelhoch, H. 1967. Spectroscopic determination of tryptophan and tyrosine in proteins. *Biochemistry.* 6:1948–1954.
26. Osváth, S., L. Herényi, …, G. Köhler. 2006. Hierarchic finite level energy landscape model: to describe the refolding kinetics of phosphoglycerate kinase. *J. Biol. Chem.* 281:24375–24380.
27. Osváth, S., G. Köhler, …, J. Fidy. 2005. Asymmetric effect of domain interactions on the kinetics of folding in yeast phosphoglycerate kinase. *Protein Sci.* 14:1609–1616.
28. Bryan, R. K. 1990. Maximum entropy analysis of oversampled data problems. *Eur. Biophys. J.* 18:165–174.
29. Karplus, M. I., T. Ichiye, and B. M. Pettitt. 1987. Configurational entropy of native proteins. *Biophys. J.* 52:1083–1085.